  Bull. Chem. Soc. Jpn., 65, 1799—1806 (1992)

Tetrakis(thiolato)nickelate(II), $[Ni(RS)_4]^{2-}$; Ligand Dissociation and Electronic Spectra

Takeshi YAMAMURA and Hiroki ARAI
Department of Chemistry, Faculty of Science, Science University of Tokyo,
Kagurazaka, Shinjuku-ku, Tokyo 162
(Received November 12, 1991)

The dissociation feature of nickel complexes of arenethiolates, $[Ni(RS)_4]^{2-}$ (RSH=*p*-$CH_3C_6H_4SH$, *m*-$CH_3C_6H_4SH$, C_6H_5SH, *p*-ClC_6H_4SH, *p*-$NO_2C_6H_4SH$) in DMSO was studied by spectrophotometric method. ^1H NMR experiment on $[Ni(RS)_4]^{2-}$ (RSH=2,4,6-trideuteriobenzenethiol) in DMSO-d_6 revealed that this system obeys the following equilibrium scheme generating the diamagnetic nickel species, $[Ni(RS)_3(solv)]^-$ and $[Ni(RS)_2(solv)_2]$ (solv=solvent ligand). Dissociation constants K_d, K_e, and K_e' were calculated from the NMR data.

$$[Ni(RS)_4]^{2-} \underset{\text{solvent}}{\overset{K_d}{\rightleftharpoons}} [Ni(RS)_3(solv)]^- + RS^-$$

$$[Ni(RS)_3(solv)]^- \underset{\text{solvent}}{\overset{K_e(K_e')}{\rightleftharpoons}} [Ni(RS)_2(solv)_2]\ (cis,\ trans) + 2RS^-$$

Intrinsic UV-vis. absorption spectra of $[Ni(RS)_n(solv)_{4-n}]^{(n-2)-}$ ($RS^-=C_6H_5S^-$, n=2, 3, 4) were derived from the least squares fitting analyses of the absorption change data obtained under different concentrations of RS^-. The absorption spectrum of $[Ni(t\text{-}C_4H_9S)_4]^{2-}$ was also measured in solid state. Crystal field calculations for both $[Ni(C_6H_5S)_4]^{2-}$ and $[Ni(t\text{-}C_4H_9S)_4]^{2-}$ were examined. The results were compared with those of $[NiX_4]^{2-}$ (X^-=Cl^-, Br^-, I^-), as well as the nickel exchanged aspartate transcarbamoylase. The structures of $[Ni(RS)_n(solv)_{4-n}]^{(n-2)-}$ were discussed.

Nickel/thiolate systems[1-9] have the tendency to form multinuclear compounds with square planar NiS_4 coordination units, in which the thiolates, of terminal type[1,3-6] or chelating type,[7-8] take the bridging dispositions. On the other hand, the chemistry of mononuclear nickel complexes with simple thiolates(of arene or alkane type) has not been developed enough,[2,7,9] although this provides the basic knowledge for understanding the aspects of not only Ni–SR systems but also the metal/cysteinate sites of nickel enzymes[10] or nickel exchanged metal proteins such as aspartate transcarbamoylase (Ni–ATCase).[11]

We once reported a preliminary study about the ligand dissociation in $[Ni(RS)_4]^{2-}$ (RS^-; terminal ligands) in aprotic solvents.[2e] Here, we report the details of this equilibrium. The study was performed by NMR at first on the deuterio thiolato complex. Then, on the basis of this analysis, intrinsic absorption spectra of $[Ni(RS)_n(solv)_{4-n}]^{(n-2)-}$ ($RS^-=C_6H_5S^-$, n=2, 3, 4) were derived from the absorption data of the $[Ni(RS)_4]^{2-}$ under various RS^- concentrations. The ligand field of this tetrakis(benzenethiolato) complex was calculated and discussed briefly with respect to the Ni(II) in nickel exchanged aspartate transcarbamoylase.

Experimental

Every synthetic procedure and observation was carried out under argon atmosphere. The DMSO and DMF for the syntheses of arenethiolato complexes were dried over BaO and distilled under reduced pressure. Solvents for the syntheses of $(NEt_4)_2[Ni(t\text{-}C_4H_9S)_4]$, as well as for the physicochemical measurements, were dried strictly; DMSO, DMSO-d_6, DMF, and acetonitrile for this purpose were refluxed over CaH_2 for three days and distilled twice under reduced pressure; ethyl acetate was purified by refluxing with phenyl isocyanate and distilled on a helices column twice; ether was dried over $LiAlH_4$.

Physicochemical Measurements. ^1H NMR spectra were recorded on JNM-EX270L and GSF-500 spectrometers with the probe temperature regulated at 25°C. UV-vis and NIR measurements were carried out with Hitachi 228 and 3400 spectrophotometers. The absorption spectrum of $[Ni(t\text{-}C_4H_9S)_4]^{2-}$ was measured both in solid and in solution. For the solid state observation, powder (mixed in MgO for diffuse reflectance experiment) and thin film samples were prepared under argon atmosphere, and sealed in quartz cells with short optical-path length.

Materials. 2,4,6-Trideuteriobenzenethiol (2,4,6-$D_3C_6H_2SH$) was prepared from 2,4,6-$D_3C_6H_2NH_2$[12] by the usual method.[13] The thiolato nickel complexes, $(NEt_4)_2[Ni(RS)_4]$ (RSH=C_6H_5SH, *p*-$CH_3C_6H_4SH$, *p*-ClC_6H_4SH, 2,4,6-$D_3C_6H_2SH$) were prepared as described before.[2c,2e] $(NEt_4)_2[Ni(m\text{-}CH_3C_6H_4S)_4]$, $(NEt_4)_2[Ni(p\text{-}NO_2C_6H_4S)_4]$, and $(NEt_4)_2[Ni(t\text{-}C_4H_9S)_4]$ were synthesized by the following procedures. Fresh and dried sodium thiolates were used for the preparations.

$(NEt_4)_2[Ni(m\text{-}CH_3C_6H_4S_4]$: The acetonitrile slution of $(NEt_4)_2[NiCl_4]$ (11.8 g (30 mmol)/300 ml) was added dropwise to the suspension of *m*-$CH_3C_6H_4S^-Na^+$ in acetonitrile (17.5 g (120 mmol)/100 ml). The reaction mixture was stirred for several hours and passed through a glass frit to remove the insoluble materials. Then, the volume of this filtrate was reduced to 100 ml, and stood at 0°C overnight. The crystals

appeared in the solution were collected, washed with acetonitrile–ether several times and dried in vacuo at r.t. Crude yield; 10.41 g (41%). Found: C, 65.02; H, 8.44; N, 3.45%. Calcd for $C_{44}H_{68}N_2S_4Ni$: C, 65.09; H, 8.44; N, 3.45%.

$(NEt_4)_2[Ni(p\text{-}NO_2C_6H_4S)_4]$: The acetonitrile solution (300 ml) containing 11.8 g (30 mmol) of $(NEt_4)_2[NiCl_4]$ was added dropwise to the suspension of p-$NO_2C_6H_4S^-Na^+$/acetonitrile (22.4 g (120 mmol)/200 ml). After filtering off the white precipitate, the solvent was removed from the filtrate. The residue was washed with EtOH for several times and fractionally recrystallized from aceton. The final crystals were collected and washed with acetone–ethyl acetate (1 : 2). Yield 10.6 g (37.7%). Found: C, 51.48; H, 6.35; N, 8.78%. Calcd for $C_{40}H_{60}N_6O_8S_4Ni$: C, 51.13; H, 6.05; N, 8.95%.

$(NEt_4)_2[Ni(t\text{-}C_4H_9S)_4]$: $(NEt_4)_2[NiCl_4]$ (11.8 g; 30 mmol) in acetonitrile (300 ml) was added dropwise to the suspension of t-$C_4H_9S^-Na^+$ (9.61 g, 120 mmol) in acetonitrile (100 ml). This yielded immediately the purple color of the tetrakis(thiolato) nickel complex. The solution was stirred further 4 h to complete the reaction. Then, the white precipitate of NaCl which resulted in the flask was removed by filtration. The filtrate was reduced to ca. 60 ml, to which 150 ml of dried ether was added. The solution was stood at −10°C for 2 d in a refrigerator. The crystals, which appeared in the solution, were collected by filtration, washed with ether three times, and then, dried in vacuo overnight. Crude yield; 9.6 g (47.3%). Further purification was achieved by the recrystallization from acetonitrile–ether mixed solution. Found: C, 55.91; H, 11.45; N, 4.14%. Calcd for $C_{32}H_{76}N_2S_4Ni$: C, 56.86; H, 11.33; N, 4.14%.

Results

Equilibria in Solutions. UV-vis spectrum of $[Ni(C_6H_5S)_4]^{2-}$ was concentration dependent in DMSO (2.0—32.0 mM; 1 M=1 mol dm^{-3}). Similar absorption change was observed for every arenethiolate complex. Concentration dependence was observed also in the ^{1}H NMR experiment (in DMSO-d_6), which afforded two types of ring proton signals; 1) diamagnetic signals observed in the usual ring proton region, 2) contact shifted ones observed at about 21.4 ppm and −11.5 ppm.[2d] This result agrees with the Hollah's description that the magnetic susceptibility of $[Ni(C_6H_5S)_4]^{2-}$ in solution was lower than the theoretical value.[2a] If the complex in solution obeys the coordination geometry in the solid state[2a,2c,2d] (Td; S=1), only the contact shifted signals should appear. There are two ways of explanation for the appearance of the diamagnetic species; 1) association/dissociation equilibrium,[2c] and 2) tetrahedral–square planar equilibrium.[2d] It is clear that the latter mechanism proposed by Rosenfield does not explain the concentration dependence.

Visible region absorption spectrum of $[Ni(C_6H_5S)_4]^{2-}$ in DMSO does not show well resolvable maxima in diluted conditions (Fig. 1A-a; 18.4 mM; 1 M=mol dm^{-3}, optical-path length l=0.0104 cm). However, under excess amount of $C_6H_5S^-NEt_4^+$, it shows four distinguishable bands (Fig. 1A-b). The similarity berween this spectra and the solid state one (Fig. 1A-c) seems to

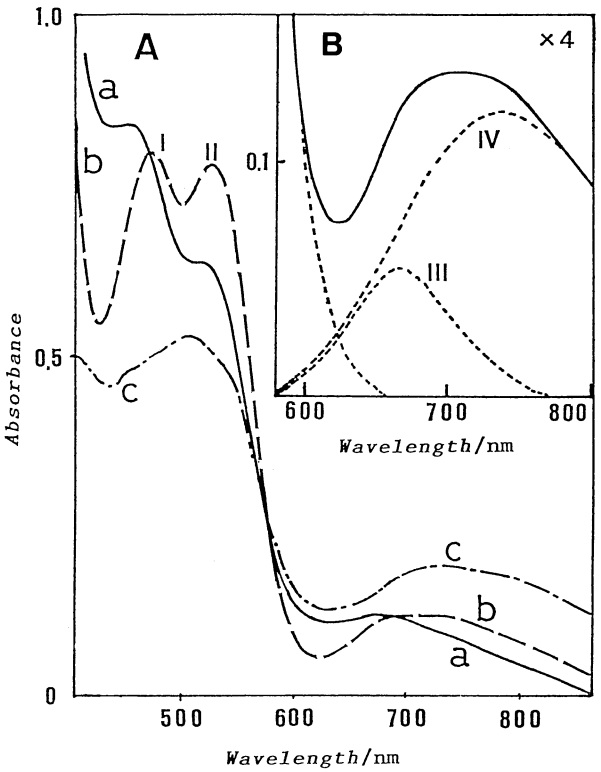

Fig. 1A. UV-vis spectra. a: $(NEt_4)_2[Ni(C_6H_5S)_4]$ in DMSO (18.4 mM, solid line), b: $(NEt_4)_2[Ni(C_6H_5S)_4]$ (18.4 mM) under $C_6H_5S^-NEt_4^+$ (92.4 mM) in DMSO (dashed line), c: thin film $(NEt_4)_2[Ni(C_6H_5S)_4]$ (dashed and dotted line). 0.0104 cm optical-path length cell was used for a and b.

Fig. 1B. The expansion of Fig. 1A-b at 600—800 nm region (the solid line), and the result of its deconvolution (dashed lines; Gaussian line shapes were assumed for ε/cm^{-1}).

suggest that some dissociation equilibrium including $[Ni(C_6H_5S)_4]^{2-}$ and $C_6H_5S^-$ undergoes in the solution.

The detail of this equilibrium was studied by ^{1}H NMR (500 MHz and 270 MHz, in DMSO-d_6). In order to simplify the ring proton signals, and thereby to clarify the equilibrium scheme, an experiment on the complex of o- and p-deuterated benzenethiol, $[Ni(2,4,6\text{-}D_3C_6H_2S)_4]^{2-}$, was examined. The ring proton and the low field (20—25 ppm) regions of 500 MHz ^{1}H NMR observed for 14.2—106.0 mM solutions are shown in Fig. 2. As is seen here, the ring proton region involves five peaks **a**—**e**, whereas the low field region involves one peak (**t**; 21.40 ppm). This isotope experiment leads to the conclusion that the 21.44 ppm signal observed for the $[Ni(C_6H_5S)_4]^{2-}$ solution is originating from the m-ring proton of some paramagnetic species which appeared in the solution. Comparing the signals of Fig. 2A (14.2 mM; **a** 7.000 ppm, **b**; 6.988 ppm, **c**; 6.956 pm, **d**; 6.813 ppm, **e**; 6.640 ppm) with those of the related compounds, 2,4,6-$D_3C_6H_2S^-$ (6.64 ppm), 2,4,6-$D_3C_6H_2SH$ (7.13 ppm) and $(2,4,6\text{-}D_3C_6H_2S^-)_2$ (7.28 ppm),[14] signal is

assigned to the *m*-proton of 2,4,6-$D_3C_6H_2S^-$.[15]

Figure 2 depicts the ^1H NMR spectra of $[Ni(RS)_4]^{2-}$, RS^-=2,4,6-$D_3C_6H_2S^-$, under various concentrations. All the peaks shown here were observed to shift slightly (<0.1 ppm) to high field upon dilution (see the figure caption). The addition of a large amount (70 equiv) of 2,4,6-$D_3C_6H_2S^-$ (corresponds to peak **e**) to the diluted solution of the nickelate (3.6 mM) enhanced the signal intensity of **t** to the theoretical amount, while quenched all of the diamagnetic ring protons except **e**. Considering this and the result of the absorption experiment, now it is possible to conclude that 1) $[Ni(C_6H_5S)_4]^{2-}$ in DMSO eliminates $C_6H_5S^-$ in an equilibrium manner generating diamagnetic nickel complexes.

In order to reveal the details of the equilibrium, further calculation was examined. Table 1 summarizes the proton numbers of **a**—**e**. This table and Fig. 2 clarifies three points: 1) the relative proton numbers of **a**+**b**+**c**+**d** and **e** increase with dilution, whereas **t** decreases; 2) the ratio (**a**+**b**+**c**+**d**)/**e** diminishes upon dilution. 3) Intensity change of peak **b**, which is the largest among **a**—**d**, is the smallest. These results seem to indicate the successive dissociation of the free thiolate and, at the same time, the outgrowth of some diamagnetic species from the tetrakes(thiolato) complex upon dilution.

The practical concentrations of $[Ni(2,4,6\text{-}D_3C_6H_2S)_4]^{2-}$, C_4, and 2,4,6-$D_3C_6H_2S^-$, S, were calculated from the proton numbers of **t** and **e**, respectively, and the total concentration of Ni^{2+}, C_0. Possible reaction schemes were searched on these practical concentrations and the proton numbers of **a**—**d** in Table 1. The final result is written as Scheme 1 (Possibility for the other cases will be discussed later).

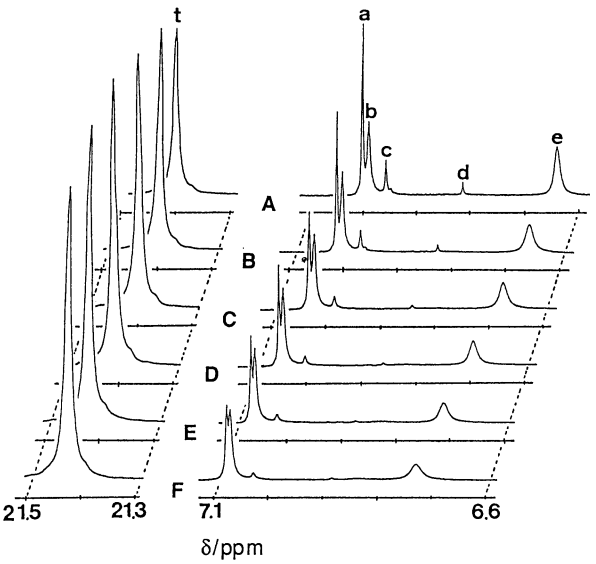

Fig. 2. Concentration dependence of the 500 MHz ^1H NMR spectra of $(NEt_4)_2[Ni(2,4,6\text{-}D_3C_6H_2S)]$ in DMSO-d_6 (28°C) at 21.3—21.5 and 6.7—7.1 ppm regions. The concentrations are: A; 14.2 mM, B; 29.3 mM, C; 49.2 mM, D; 74.2 mM, E; 91.6 mM, F; 106 mM. Peak shift observed in this concentration region are; **a**: 7.000—7.074 ppm, **b**: 6.988—7.068 ppm, **c**: 6.956—7.026 ppm, **d**: 6.813—6.859 ppm, **e**: 6.640—6.728 ppm, **t**: 21.399—21.420 ppm.

$$[Ni(RS)_4]^{2-} \overset{K_d}{\rightleftharpoons} [Ni(RS)_3(solv)_q]^- + RS^-$$

$$\overset{K_e, K_e'}{\rightleftharpoons} [Ni(RS)_2(solv)_r]\ (cis,\ trans) + 2RS^-$$

Scheme 1. (RS^-=2,4,6-$D_3C_6H_2S^-$)

Almost all of the nickel species generated from the tetrakis(thiolato) complex are diamagnetic. This is approximately true, because the sum of the ring proton numbers observed as **t**, **a**, **b**, **c**, **d**, and **e** distributes within 7.65—7.96. This is close to the theoretical value, 8.[16] These diamagnetic species should be mononuclear. The possibilities of the formation of diamagnetic condensates such as $[Ni_2(RS)_6]^{2-}$ and $[Ni_3(RS)_8]^{2-}$,[3,7a] were excluded from the view point of mass action law. In practice, calculations assuming these types of comounds afforded no constant K_d independent on C_0. Formation of adamantane like $[Ni_4(RS)_{10}]^{2-}$,[17] which would be paramagnetic in expectation, and, is still unknown for nickel, is improbable by the same reason. Any efforts to find the other dissociation/association scheme that satisfies (**a**+**b**+**c**+**d**)/**e**=2—3 were all unsuccessful.

As will be discussed later, the mononuclear nickel species are reliably square planar because of their diamagnetism. Hence, q=1 and r=2 are derived for $[Ni(2,4,6,\text{-}D_3C_6H_2S)_3(solv)_q]^-$ and $[Ni(2,4,6,\text{-}D_3C_6H_2S)_2$-

Table 1. Numbers of *m*-Ring Protons of the Paramagnetic Complex (t), the Diamagnetic Complexes (**a**, **b**, **c**, **d**, **e**), and the Free Thiolate (**e**) Corrected for the Number of Ammonium Methyl Proton (=24)

No.	C_0/mM[a]	NMe_4^+	t	a	b	c	d	e	(a+b+c+d)/e[b]
1	14.2	24	3.85	1.05	1.24	0.26	0.07	1.31	2.01
2	29.3	24	4.80	0.76	1.17	0.14	0.03	1.02	2.05
3	49.2	24	5.13	0.59	1.09	0.01	0.02	0.81	2.22
4	74.2	24	5.45	0.52	0.97	0.07	0.02	0.69	2.26
5	91.6	24	5.84	0.49	0.93	0.07	0.02	0.58	2.60
6	106.0	24	5.87	0.54	0.79	0.09	0.02	0.55	2.65

a) C_0=Total concentration of Ni^{2+}. b) The ideal value for (**a**+**b**+**c**+**d**)/**e** is 3 at the limit of high concentration.

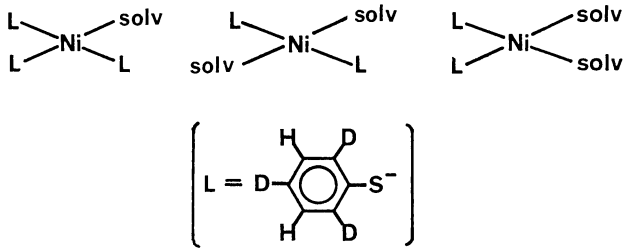

Fig. 3. Situations of *m*-ring protons in $[Ni(RS)_3(solv)]^-$ and $[Ni(RS)_2(solv)_2]$; RS^-=2,4,6-$D_3C_6H_2S^-$.

$(solv)_r]$, respectively. The former includes two kinds (*cis* and *trans*) of thiolato ligands according to the solvent as ligand, whereas the latter includes *cis* and *trans* isomers (Fig. 3). As the result, four types of diamagnetic ring protons are expected to appear in the ^1H NMR chart for slow exchange case. Based on this consideration, and, in order to obtain consistent result, we further proposed that peak **a** involved two kinds of protons accidentally: one from the "*trans*" thiolato ligand of $[Ni(2,4,6\text{-}D_3C_6H_2S)_3(solv)]^-$, which includes two protons, and the other from one of the isomers of $[Ni(2,4,6\text{-}D_3C_6H_2S)_2(solv)_2]$, which includes four protons (Fig. 3). In consequence, the concentration of $[Ni(2,4,6\text{-}D_3C_6H_2S)_3(solv)]^-$, C_3, was calculated from the proton number of peak **b** as corresponding to the four protons of the two "*cis*" thiolato ligands. On the other hand, the concentration of *cis* and *trans* $[Ni(2,4,6\text{-}D_3C_6H_2S)_2(solv)_2]$, C_2 and C_2', were calculated from the proton numbers of **c** and **a**−**b**/2. From these concentrations, the equilibrium constants K_d, K_e, and K_e' were derived. The results are listed also in Table 2.

Starting from their mean values (Table 2), K_d, K_e, and K_e' were further refined by simulating the observed concentrations, S, C_4, C_3, C_2, and C_2'. In this simulation, the concentration of RS^- (S) was calculated by Eq. 1,

$$S^3+(-S_0+K_d)S^2+(-S_0-C_0+K_e+K_e')K_dS -(S_0+2C_0)K_d(K_e+K_e')=0 \quad (1)$$

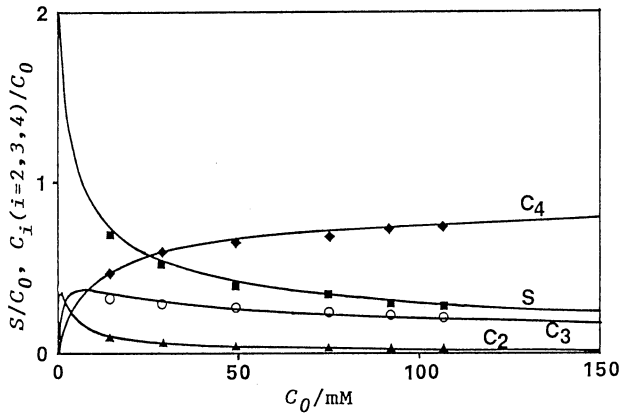

Fig. 4. The rises and decays of C_4/C_0, C_3/C_0, C_2/C_0, C_2'/C_0 (C_4, C_3, C_2=C_2', and S are the practical concentrations of $[Ni(RS)_4]^{2-}$, $[Ni(RS)_3(solv)]^-$, $[Ni(RS)_2(solv)_2]$, and RS^-, respectively. C_0 is the total concentration of Ni^{2+}. RS^- used here is $C_6H_5S^-$). ■, ◆, ○, ▲; obtained from ^1H NMR data. Solid line (−); calculated for K_d=7.8 mM, K_e=K_e'=3.0 mM.

where S_0 means the concentration of the RS^- added to the solution. C_4, C_3, C_2 and C_2', too, were calculated similarly. The rises and decays of C_4/C_0, C_3/C_0, C_2/C_0, and C_2'/C_0 simulated by changing K_d, K_e=K_e' (this seems reasonable from Table 2) are shown in Fig. 4[18] as the functions of C_0. As is seen here, the refined values (K_d=7.8 mM and K_e=K_e'=3.0 mM) reproduces well the experimental result.[19]

The ratios C_2/C_4, C_2'/C_4, C_2/C_3, and C_2'/C_3 in the above case are less than 0.05 for the concentration region of C_0>50 mM. This means that the equilibrium reaction scheme is approximately given by Scheme 2 for a comparatively higher concentration solution. The equilibrium constants of

$$[Ni(RS)_4]^{2-} \overset{K_d}{\rightleftharpoons} [Ni(RS)_3(solv)]^- + RS^-$$

Scheme 2.

Table 2. Practical Concentrations of $[Ni(RS)_4]^{2-}$ (C_4), $[Ni(RS)_3(solv)_q]^-$ (C_3), $[Ni(RS)_2(solv)_r]$ (C_2, C_2'), and RS^- (S); RS^-=2,4,6-$D_3C_6H_2S^-$, and the Equilibrium Constants K_d, K_e, and K_e' (Scheme 1) Obtained from These Practical Concentrations

No.	C_0/mM[a]	C_4/mM[b]	C_3/mM[c]	C_2/mM[d]	C_2'/mM[e]	S/mM[f]	K_d/mM[g]	K_e/mM[h]	K_e'/mM[i]
1	14.2	6.8	4.4	1.5	0.9	9.3	6.0	3.2	1.9
2	29.3	17.6	8.6	1.3	1.0	14.9	7.3	2.2	1.8
3	49.2	31.5	13.4	0.6	1.2	19.8	8.4	0.9	1.8
4	74.2	50.5	17.9	0.7	1.2	25.7	9.1	1.1	1.8
5	91.6	66.9	21.2	1.4	1.7	26.6	8.4	1.8	2.1
6	106.0	77.8	21.0	3.8	2.4	29.0	7.8	1.2	2.2
						Mean	7.8	1.7	1.9

a) C_0=total concentration of Ni^{2+} (1 M=1 mol dm^{-3}). b) The concentration of $[Ni(RS)_4]^{2-}$; derived from the number of peak **t**. c) The concentration of $[Ni(RS)_3(solv)_q]^-$; derived from the number of peak **b**. d) The concentration of $[Ni(RS)_2(solv)_r]$; calculated from the proton number, (**a**−**b**/2). e) The concentration of the $[Ni(RS)_2(solv)_2]$ isomer; calculated from the proton number of peak **c**. f) The concentration of RS^-; calculated from the proton number of peak **e**. g) $K_d=C_3\cdot S/C_4$. h) $K_e=C_2\cdot S/C_3$. i) $K_e'=C_2'\cdot S/C_3$.

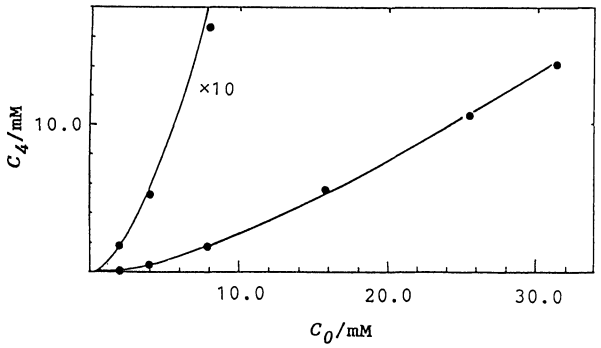

Fig. 5. The practical concentration of $[Ni(RS)_4]^{2-}$ (C_4) vs. total concentration of Ni^{2+} (C_0); RS^-=*p*-$CH_3C_6H_4S^-$. Solid circles (●); obtained from ^1H NMR data. Solid line (—); calculated from $K_d=(C_0-C_4)^2/C_4$, K_d=20.8 mM.

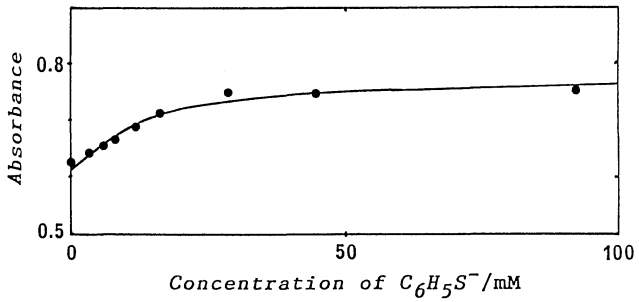

Fig. 6. Simulation of the absorbance change of $[Ni(C_6H_5S)_4]^{2-}$/DMSO at 520 nm for various S_0 values. Solid circles (●); observed with 0.0104 cm optical-path length cell, C_0 (total Ni^{2+} concentration)=18.4 mM. S_0 (the concentration of $RS^-=C_6H_5S^-$ added to the solution)=0, 3.26, 5.69, 7.78, 11.7, 16.2, 28.5, 44.6, 92.4 mM. Solid line (—); obtained for ε_4=4058, ε_3=3154, $\varepsilon_2=\varepsilon_2'$=3266 M^{-1} cm^{-1}.

usual nondeuterio arenethiolato complexes were roughly obtained based on this simplified scheme, as we reported before.[2e] Since the ring proton signals of these cases were not discriminated like those of the 2,4,6-$D_3C_6H_2S^-$ experiment, the approximate numbers of the diamagnetic ring protons were calculated from the paramagnetic *m*-proton intensities.[20] K_d (20.8 mM) thus obtained for RS^-=*p*-$CH_3C_6H_4S^-$ case reproduces well the profile of the relative concentration of paramagnetic $[Ni(p\text{-}CH_3C_6H_4S)_4]^{2-}$, C_4, to the total nickel concentration, C_0 (See Fig. 5). The equilibrium constants for the other arenethiolate complexes are as follows (K_d/mM): $[Ni(p\text{-}CH_3C_6H_4S)_4]^{2-}$; 21.0 $[Ni(m\text{-}CH_3C_6H_4S)_4]^{2-}$; 12.5, $[Ni(C_6H_5S)_4]^{2-}$; 7.0, $[Ni(p\text{-}ClC_6H_4S)_4]^{2-}$; 2.6, $[Ni(p\text{-}NO_2C_6H_4S)_4]^{2-}$; 9.5. It should be noticed that K_d=7.0 mM[21] thus obtained for $[Ni(C_6H_5S)_4]^{2-}$ is close to the value obtained from the deuterium experiment (7.8 mM) in spite of the innacuracy of the former method.

Intrinsic Absorption Spectra. Intrinsic absorption spectra of $[Ni(RS)_4]^{2-}$ and $[Ni(RS)_3(sol)]^-$ (and also $[Ni(RS)_2(solv)_2]$; *cis* and *trans*) for $RS^-=C_6H_5S^-$ were estimated as follows based on Scheme 2. If we adopt Scheme 2, the absorbance of the solution at an arbitrary wavelength (>350 nm) point is written by Eq. 2; where ε_4, ε_3, ε_2, and ε_2' are the extinction coefficients of $[Ni(RS)_4]^{2-}$, $[Ni(RS)_3(sol)]^-$, and $[Ni(RS)_2(sol)_2]$ (*cis* and *trans*), respectively, and l is the optical-path length. C_4, C_3, C_2, and C_2' are the functions of S, which is calculated from

$$\text{Absorbance}/l=\varepsilon_4C_4+\varepsilon_3C_3+\varepsilon_2C_2+\varepsilon_2'C_2' \quad (2)$$

Eq. 1. The absorbance change at 520 nm for $[Ni(C_6H_5S)_4]^{2-}/C_6H_5S^-$ (C_0=18.4 mM, l=0.0104 cm, in DMSO) is shown in Fig. 6 (solid circles) as the function of S_0 (0—92.4 mM). This result was simulated by least squares fitting varying ε_4, ε_3, and $\varepsilon_2=\varepsilon_2'$[22] ($K_d$ and $K_e=K_e'$ were fixed at 7.80 and 3.00 mM, respectively). The best fit (Fig. 6; solid line) afforded ε_4=4058, ε_3=3154, $\varepsilon_2=\varepsilon_2'$=3266 M^{-1} cm^{-1}. This curve fitting was applied for every 20 nm wavelength point in between 440 and 800 nm, which afforded the absorption profiles of the $[Ni(RS)_4]^{2-}$, $[Ni(RS)_3(solv)]^-$, and $[Ni(RS)_2(solv)_2]$ (*cis* and *trans*) in molar absorptivity. Comparison of these estimated spectra with the raw spectra in Fig. 1A revealed that the raw spectrum under diluted condition (Fig. 1A-a) represents the sum of the spectra of the $[Ni(RS)_3(solv)]^-$ and $[Ni(RS)_2(solv)_2]$ (*cis* and *trans*) with more than 99.5% purity, whereas the raw spectrum under 92.4 mM of the common thiolate (Fig. 1A-b) includes 95.6% tetrahedral $[Ni(RS)_4]^{2-}$.

As for NIR region, the addition of $C_6H_5S^-$ to the solution did not cause the appearance of new peaks, as did in vis. region, but increased the whole absorbance. The accurate estimation of the true absorbance by the method of the vis. region mentioned above was impossible in this region, because the addition of much amount (>5 equiv) of $C_6H_5S^-$ caused the appearance of some combined vibrational mode of benzen ring just at the absorption maximum of $[Ni(C_6H_5S)_4]^{2-}$. However, though innacurate, the analysis clearly showed no absorption assignable to any of $[Ni(RS)_3(solv)]^-$ and $[Ni(RS)_2(solv)_2]$. The feature was observed for the other arenethiolate cases also.

Crystal Field Calculation. Figure 1B shows the d–d transition region of the 95.6% purity $[Ni(C_6H_5S)_4]^{2-}$ in DMSO (see above). The dashed lines in this figure shows the Gaussian deconvolution. As is seen in this figure, the true absorption of tetrahedral $[Ni(C_6H_5S)_4]^{2-}$ has characteristic geminal absorption maxima in 600—800 nm region (band III at 666 nm and IV at 740 nm). These two bands were observed for the other arenethiolate complexes except for $[Ni(p\text{-}NO_2C_6H_4S)_4]^{2-}$.

The absorption maxima of $[Ni(RS)_4]^{2-}$, $RS^-=C_6H_5S^-$ and t-$C_4H_9S^-$ [23] are listed in Table 3 with those of the nickel exchanged aspartate transcarbamoylase (Ni–

Table 3. Observed Absorption Maxima of $[Ni(RS)_4]^{2-}$ (RSH=*p*-$CH_3C_6H_4S^-$; **1**, *t*-$C_4H_9S^-$; **2**) and the Results of the Crystal Field Calculations Based on Liehr and Ballhausen[26] (Calculation for Ni–ATCase[11a] is listed also)

Compound	Band	Observed λ_{max}/cm^{-1}	Calcd[h,i,j] λ_{max}/cm^{-1}
		15060	
	$h\nu_3$[d]	13590 (ε 625), 13157	13850, 13709, 13313, 13251; (13530)[k]
1[a]	(A)[e]	—	10737, 9438
	$h\nu_2$[f]	7840 (ε 12.4)	9173
	$h\nu_1$[g]	5405 (ε 170)	5644, 5380, 5317, 5280; (5405)[k]
	$h\nu_3$[d]	12200	12377, 12206, 11921, 11847; (12088)[k]
2[b]	(A)[e]	9090	9548, 9236; (9392)[k]
	$h\nu_2$[f]	6450	6465
	$h\nu_1$[g]	—	3637, 3523, 3338, 3316; (3454)[k]
		15040	
Ni–ATCase[c]	$h\nu_3$[d]	13890	14251, 14120, 13716, 13653; (13935)[k]

a) $[Ni(p\text{-}CH_3C_6H_4S)_4]^{2-}$ in DMSO under the presence of 100 equiv of *p*-$CH_3C_6H_4S^-$ (see Fig. 1B). b) $[Ni(t\text{-}C_4H_9)_4]^{2-}$, diffuse reflectance spectrum. c) Ni–ATCase.[11a] d) $\Gamma_1(^3P_0)$, $\Gamma_5(^2P_2)$, $\Gamma_4(^3P_1)$, $\Gamma_3(^3P_2)$; allowed. e) $\Gamma_3(^1D_2)$, $\Gamma_5(^1D_2)$; forbidden. f) $\Gamma_5(^3F_4)$; allowed. g) $\Gamma_2(^3F_3)$, $\Gamma_4(^3F_3)$, $\Gamma_3(^3F_2)$, $\Gamma_5(^3F_2)$, $\Gamma_5(^3F_3)$; allowed. h) **1**, calcd for F_4 (Slater–Condon parameter)=65 cm^{-1}, D_q=525 cm^{-1}. i) **2**, calcd for F_4=67 cm^{-1} and D_q=300 cm^{-1}. j) Ni-ATCase, calcd for F_4=65 cm^{-1} and D_q=575 cm^{-1}. k) Average value.

Table 4. Crystal Field Parameters for $[NiX_4]^{2-}$

$[MX_4]^{2-}$	$10D_q/cm^{-1}$	B'[a]	β[b]
$[Ni(p\text{-}CH_3C_6H_4S)_4]^{2-}$[c]	5250	585	0.568
$[Ni(t\text{-}C_4H_9)_4]^{2-}$[c]	3000	603	0.585
Ni–ATCase[c]	5750	585	0.568
$[NiCl_4]^{2-}$[d]	3580	746	0.724
$[NiBr_4]^{2-}$[d]	3380	691	0.671
$[NiI_4]^{2-}$[d]	3350	572	0.555
$[Co(C_6H_5)_4]^{2-}$[e]	4030	643	
$[Co(S_2\text{-}o\text{-}xyl)_2]$[e]	4090	619	
$[Co(CAAC)_2]^{2-}$[f]	4520	591	

a) Racah parameter. b) $\beta=B'/B$, B is the Racah parameter for the free Ni(II) ion (1030 cm^{-1}). c) This work. d) Ref. 24. e) S_2-*o*-xyl=*o*-xylene-α,α'-dithiolate, Ref. 8a. f) CAAC=*Z*-Cys–Ala–Ala–Cys–OMe.[36]

ATCase).

The bands for $[Ni(C_6H_5S)_4]^{2-}$ and Ni–ATCase were assigned according to ν_1, ν_2, and ν_3 of the ordinary tetrahedral nickel cases,[24] as well as those for Bis(imidophosphinato)nickel(II), which also shows tetrahedral NiS_4 geometry.[25] On the other hand, the bands for $[Ni(t\text{-}C_4H_9S)_4]^{2-}$ were not explained by the same manner as will be shown later. Crystal field calculation were carried out by using Ballhausen and Liehr's method,[26] which is known to rationalize d–d transitions well. Obtained $10D_q$ and Racah parameters, $B'=9F_4(F_4=$ Slater–Condon–Shortley parameter), are listed in Table 4, with those of $[NiX_4]^{2-}$ ($X^-=C^-$, Br^-, and I^-),[24] as well as those of tetrahedral Co^{2+} thiolates,[8a] for comparison. Our calculation for $[Ni(RS)_4]^{2-}$ ($RS^-=C_6H_5S^-$ and *t*-$C_4H_9S^-$) has clarified four points. 1) Thiolate ligand belongs to weak ligand,[8a,27,28] although a fairly large D_q (525 cm^{-1}) and low Racah parameters (B'=585 cm^{-1} or F_4=65 cm^{-1}; indicates the increased Ni–S covalency in the compound) were necessary to explain the result for $[Ni(C_6H_5S)_4]^{2-}$ insofar as we depend on the usual assignment.[24,25] 2) Band III of $[Ni(C_6H_5S)_4]^{2-}$ (see Fig. 1B) could not be interpreted within crystal field theory. 4) The bands for $[Ni(t\text{-}C_4H_9S)_4]^{2-}$ were best explained on the assumption that D_q=300 cm^{-1} and B'=603 cm^{-1}. This weak crystal field would be the result of the strong repulsion among *t*-$C_4H_9S^-$ anions on the nickel.

Discussion

Ligand Dissociation. Ligand dissociation is commonly seen for tetrahedral nickelate with four anionic ligands. $[NiX_4]^{2-}$ (X=Cl, Br, I), for instance, are known to dissociate one of the ligands in polar solvents. Snyder et al. suggested that $[Ni(edt)_2]^{2-}$ ($edtH_2$=1,2-ethanedithiol, $HSCH_2CH_2SH$) spontaneously eliminates one of its edt^{2-} in aprotic media to assemble in the dinuclear condensate, $[Ni_2(edt)_3]^{2-}$.[7a] Ligand dissociation and the subsequent assembly seems to be characteristic to nickel thiolate in polar aprotic media. The equilibria between $[Ni_2(RS)_6]^{2-}$ and $[Ni_3(RS)_8]^{2-}$ (RS^-=EtS$^-$ and 1/2edt^{2-}) reported by Holm[3,7a] and Tremel[8b] are the examples of such scheme. It was pointed out for some cases that the dissociation/association equilibria were promoted by a negligible amount of H^+.[5b,6,7a,29] However, the system investigated here was not dependent on H^+. That is to say, the addition of water to a diluted $[Ni(C_6H_5S)_4]^{2-}$/DMSO solution (3.6 mM) caused no change to the ^1H NMR

signal. Therefore, the equilibrium found here is characteristic to nickel/arenethiolate system.

The equilibrium constant K_d showes a linear correlation to Hammet's σ parameter of the thiols. This means that the stability of nickel thiolate increases with the electron acceptance of the ligand.[30]

Coordination Geometry of $[Ni(RS)_3(solv)_q]^-$ and $[Ni(RS)_2(solv)_r]^-$. Coordination geometries of $[Ni(RS)_3(solv)_q]^-$ and $[Ni(RS)_2(solv)_r]^-$ ($RS^-=C_6H_5S^-$) are estimated from their absorption features in UV-vis and NIR regions and diamagnetism.

Low-spin nickel(II) complexes exist in square planar and five-coordinate (either trigonal bipyramidal or square pyramidal) geometries. Monosolvated $[Ni(RS)_3(solv)]^-$ in square planar geometry is the most plausible candidate for the tris(thiolato) complex. On the other hand, disolved $[Ni(RS)_3(solv)_2]^-$, which belongs to five coordination, has both possibility for diamagnetism and paramagnetism. Crystal field calculation for d^8 configuration in trigonal bipyramid geometry was performed by Becker et al. both at weak and strong field limits.[31] According to them, strong field ($D_q>2400\ cm^{-1}$) is desired for spin pairing in the ground state of this geometry. Square pyramidal geometry also requires a strong field for spin-pairing in the ground state.[32] These calculations assume low nephelauxetic effect. Slater–Condon–Shortley parameters used in these calculations ($F_4=87\ cm^{-1}$, $F_2=1250\ cm^{-1}$) were larger than our result for $[Ni(C_6H_5S)_4]^{2-}$. The reduction of F_4 and F_2 in our compounds would allow spin-pairing under smaller D_q values. In addition, the crystal field splitting of $[Ni(RS)_3(solv)_2]^-$ would be larger than that of $[Ni(RS)_4]^{2-}$, because the Coulombic repulsion among the anionic ligands of the former is weaker than the latter.[33] This will increase the possibility of spin pairing in the ground state of $[Ni(RS)_3(solv)_2]^-$. Nevertheless, the discrepancy between $D_q=525\ cm^{-1}$ and $D_q=2400\ cm^{-1}$ seems to be too large. Thus, disolvated complex $[Ni(RS)_3(solv)_2]^{1-}$ should be excluded inasmuch as we stand on crystal field theory. Simple planar complex, $[Ni(C_6H_5S)_3]^-$, which is homologous to the trigonal planar complexes such as $[Cu(C_6H_5S)_3]^-$,[34] and $[Hg(t\text{-}C_4H_9S)_3]^-$ [35] should also be excluded as situating on the extrapolate of tbp geometry. Furthermore, this type of compounds are still not known for nickel, then, it is impossible to compare the spectra with each other.

Consequently, the monosolvated square planar complex, $[Ni(RS)_3(solv)]^-$, is the most possible candidate for the diamagnetic tris(thiolato) complex. By the same reason the bis(thiolato) complexes, $[Ni(RS)_2(solv)_2]^-$ (*cis* and *trans*), will have square planar geometries, too.

Absorption Spectra of Ni-ATCase. $[Ni(C_6H_5S)_4]^{2-}$ has two absorption maxima at around 600—800 nm (Fig. 1B, band III and band IV). This geminal pattern is also seen in the absoption spectrum of Ni–ATCase (see Fig. 2 in Ref. 11a)). Although zinc site of ATCase itself takes tetrahedral geometry,[11b] there has been no evidence for the conservation of the coordination geometry and the protein folding upon the metal exchange from Zn to Ni. The observed parallelism in absorption feature between these two systems suggests strongly that the metal site in Ni–ATCase is still conserving the geometry as well as the protein folding.

In the crystal field calculation of Ni–ATCase, we fixed the Racah parameter B' at $585\ cm^{-1}$ (the same value as $[Ni(C_6H_5S)_4]^{2-}$) refering the fact that the Racah parameters for tetrahedral Co^{2+} thiolates are distributed within a narrow range for different typese of thiolates such as benzenethiolate, *o*-xylene-α,α'-dithiolate, or cysteinate.[8a,36] On this assumption, the crystal field strength of Ni–ATCase was calculated as $D_q=575\ cm^{-1}$ (Table 3,4).

References

1) a) E. W. Abel and B. C. Crosse, *J. Chem. Soc. A,* **1966**, 1377. b) P. Woodward, L. F. Dahl, E. W. Abel, and B. C. Crosse, *J. Am. Chem. Soc.,* **87**, 5252 (1965).

2) a) D. G. Hollah and D. Coucouvanis, *J. Am. Chem. Soc.,* **97**, 6917 (1975). b) D. Swenson, N. C. Baenziger, and D. Coucouvanis, *ibid.,* **100**, 1932 (1978). c) T. Yamamura, H. Miyamae, Y. Katayama, and Y. Sasaki, *Chem. Lett.,* **1985**, 269. d) S. Rosenfield, W. H. Armstrong, and P. K. Mascharak, *Inorg. Chem.,* **25**, 3014 (1986). e) T. Yamamura, *Chem. Lett.,* **1986**, 801.

3) A. D. Watson, Ch. Pulla-Rao, J. R. Dorfman, and R. H. Holm, *Inorg. Chem.,* **24**, 2820 (1985).

4) a) W. Gaete, J. Ros, X. Solans, M. Font-Altaba, and J. L. Brianso, *Inorg. Chem.,* **23**, 39 (1984). b) M. Kriege and G. Henkel, *Z. Naturforsch., B: Anorg. Chem., Org. Chem.,* **42**, 1121 (1987).

5) a) R. O. Gould and M. M. Harding, *J. Chem. Soc. A,* **1970**, 875. b) T. Yamamura, *Bull. Chem. Soc. Jpn.,* **61**, 1975 (1988). c) H. Miyamae and T. Yamamura, *Acta Crystallogr., Sect. C,* **44**, 606 (1988).

6) I. G. Dance, M. L. Scudder, and R. Secomb, *Inorg. Chem.,* **24**, 1201 (1985).

7) a) B. S. Snyder, Ch. Pulla-Rao, and R. H. Holm, *Aust. J. Chem.,* **39**, 963 (1986). b) Ch. Pulla-Rao, J. R. Dorfman, and R. H. Holm, *Inorg. Chem.,* **25**, 428 (1986).

8) a) R. W. Lane, J. A. Ibers, R. B. Frankel, G. C. Papaefthymiou, and R. H. Holm, *J. Am. Chem. Soc.,* **99**, 84 (1977). b) W. Tremel, B. Krebs, and G. Henkel, *Angew. Chem.,* **96**, 604 (1984). c) W. Tremel, M. Kriege, B. Krebs, and G. Henkel, *Inorg. Chem.,* **27**, 3886 (1988).

9) a) T. Yamamura, H. Kurihara, R. Kuroda, and N. Nakamura, *Chem. Lett.,* **1990**, 101. b) S. Fox, A. Silver, and M. Millar, *J. Am. Chem. Soc.,* **112**, 3218 (1990). c) T. Yamamura, H. Arai, H. Kurihara, and R. Kuroda, *Chem. Lett.,* **1990**, 1975.

10) J. R. Lankaster, Jr., "The Bioinorganic Chemistry of Nickel," VCH Publishers, Inc., New York (1988).

11) a) R. S. Jonson and H. K. Schachman, *Proc. Natl. Acad. Sci. U.S.A.,* **77**, 1995 (1980). b) H. L. Monaco, J. L. Crawford, and W. N. Lipscomb, *ibid.,* **75**, 5276 (1978).

12) A. P. Best, *J. Chem. Soc.,* **1946**, 239.

13) D. S. Tarbell and D. K. Hukushima, *Org. Synth.,* **3**, 809 (1955).

14) Observed with JNM-270L.

15) The slight shift from 6.64 ppm of pure 2,4,6-$D_3C_6H_2S^-$ to 6.68 ppm of that in $[Ni(2,4,6\text{-}D_3C_6H_2S)_4]^{2-}$ solution will be explained by the paramagnetism of tetrahedral $[Ni(2,4,6\text{-}D_3C_6H_2S)_4]^{2-}$ in the solution.

16) This slight defect of the ring proton number from 8 would be the result of the mixing of some unknown paramagnetic species.

17) a) T. Costa, J. R. Dorfman, K. S. Hagen, and R. H. Holm, *Inorg. Chem.*, **22**, 4091 (1983). b) K. S. Hagen, D. W. Stephan, and R. H. Holm, *Inorg. Chem.*, **21**, 3928 (1982). c) I. G. Dance and J. C. Calabrese, *J. Chem. Soc., Chem. Commun.*, **1975**, 762. d) J. L. Hencher, M. Kahn, F. F. Said, and D. G. Tuck, *Inorg. Nucl. Chem. Lett.*, **17**, 287 (1981).

18) C_4/C_0, C_3/C_0, C_2/C_0, C_2'/C_0 are given by the next equations. $C_4/C_0=S_2/U$, $C_3/C_0=K_dS/U$, $C_2/C_0=K_dK_e/U$, $C_2'/C_0=K_dK_e'/U$, where $U=S^2+K_dS+K_d(K_e+K_e')$.

19) It should be pointed out that the refined K_d, K_e, and K_e' after least squares fitting, where these are varied as the parameters, are, needless to say, different from the starting values (K_d=7.8, K_e=1.7, K_e'=1.9 mM). The agreement of K_ds obtained here suggets the consistency of the treatment based on Scheme 1 and Eq. 1. Slight increase of K_e and K_e' from 1.7 and 1.9 mM, respectively, to 3.0 mM after the fitting will be brought onto these parameters to adjust the concentrations C_4, C_3, and S (they are dominant in the equibrium) best. Additionally saying, the theoretical curve obtained by using K_d=7.8, K_e=1.7, K_e'=1.9 mM almost overlapped with the curve in Fig. 4.

20) The dissociation constants for ordinary arenethiolates were calculated by equation $K_d=(C_0-C_4)^2/C_4$, where C_0 is the total concentration of Ni^{2+}, and, C_4 the practical concentration of paramagnetic $[Ni(RS)_4]^{2-}$, which was estimated from the number of the *m*-ring proton observed at about 20 ppm.

21) We had reported K_d=4.35 for $[Ni(C_6H_5S)_4]^{2-}$ in the previous paper.[2e] According to the new experiment carefully performed than before, the value was corrected to 7.0 from 4.35.

22) Here, we assumed $\varepsilon_2=\varepsilon_2'$ for simplicity. The inherency of the calculation is not missing by this assumption because of the small contribution of Bis(thiolato) complexes in the equilibrium and the similarlity of the coordination geometry of these compounds.

23) Only the solid state (diffuse reflectance) absorption spectra are listed in Table 3 for $[Ni(t\text{-}C_4H_9S)_4]^{2-}$, because the NMR behavior of this compound was different from those of arenethiolates in aprotic media. The absorption maxima in acetonitrile (7.87 mM, 0.104 mm optical-path length) were 13100 (49), 12200 (50), 10250 ($\ll$), 6900 cm^{-1} (ε-). Those for thin layer experiment were 12130, 8770, and 6800 cm^{-1}.

24) D. M. L. Goodgame, M. Goodgame, and F. A. Cotton, *J. Am. Chem. Soc.*, **83**, 4161 (1961).

25) A. Davison and E. S. Switkes, *Inorg. Chem.*, **10**, 837 (1971).

26) A. Liehr and C. J. Ballhausen, *Ann. Phys.*, **6**, 134 (1959).

27) E. T. Lode and M. J. Coon, "Iron Sulfur Proteins," ed by W. Lovenberg, Academic Press, New York (1973), Vol. 1, pp. 173—191.

28) Crystal field calculation for tetrahedral Fe^{2+} and Co^{2+} thiolates was examined by R. H. Holm and his co-workers[8a] in terms of the site analogs of rubredoxin.[27] As the result of their calculation, they defined thiolato ligands as intrinsically weak ligand, and ranked them between Cl^- or N_3^- and nitrogen bonded SCN^- in the spectrochemical series for Co^{2+}. Our calculations on $[Ni(RS)_4]^{2-}$ systems agree with their conclusion on the ligand field strength of thiolates.

29) Dinuclear and trinuclear compounds, $[Ni_2(SEt)_6]^{2-}$ and $[Ni_3(SEt)_8]^{2-}$, were observed to condensate to $[Ni(SEt)_2]_6$. See Ref. 5b.

30) *p*-$NO_2C_6H_4S^-$ case is excluded from this tendency, probably due to the extended electron delocalization over C_6H_5- and -NO_2 moieties.

31) C. A. L. Becker, D. W. Meek, and T. M. Dunn, *J. Phys. Chem.*, **74**, 1568 (1970).

32) a) L. Sacconi, *J. Chem. Soc. A*, **1970**, 248. b) M. Ciampolini, *Inorg. Chem.*, **5**, 35 (1966).

33) Coulomic repulsion among anionic ligands increases with their number. This will weaken the crystal field splitting of the d-orbitals on the metal.

34) C. D. Garner, J. R. Nicholson, and W. Clegg, *Inorg. Chem.*, **23**, 2148 (1984).

35) S. P. Watton, J. G. Wright, F. M. MacDonnel, J. W. Bryson, M. Sabat, and T. V. O'Halloran, *J. Am. Chem. Soc.*, **112**, 2824 (1990).

36) M. Nakata, N. Ueyama, A. Nakamura, T. Nozawa, and M. Hatano, *Inorg. Chem.*, **22**, 3028 (1983).